RSC Advances

ROYAL SOCIETY OF CHEMISTRY

www.rsc.org/advances

RSC Advances

COMMUNICATION

The low dielectric constant and relaxation dielectric behavior in hydrogen-bonding metal-organic frameworks

Received 00th January 20xx,
Accepted 00th January 20xx

DOI: 10.1039/x0xx00000x

www.rsc.org/

Shan-Shan Yu,[a] Guo-Jun Yuan,[a] Hai-Bao Duan,*[a]

An 3D supramolecular hydrogen-bonding metal-organic frameworks with a formula $[Zn(CEIC)_2(H_2O)]\cdot$ 2DMF (CEIC = 4-carboxy-2-ethyl-1H-imidazole-5-carboxylate) was reported, which is a very rare example of low dielectric constant value at high temperature for the MOFs with solvent molecules. The novel dielectric relaxation of this compound was observed.

The use of low dielectric constant materials can greatly reduce the resistance-capacitance time delays, cross-talks, and power dissipation in the new generation of high-density and high-speed integrated circuits.[1,2] For faster and higher performance microelectronic devices, a new low dielectric constant material for replacing classic silicon dioxide (SiO_2) as an interlayer is needed. In addition to exhibiting low dielectric constant, these materials should posses highly crystalline nature, and offer the advantage of being microporous, with pores significantly smaller than integrated circuit (IC) features.[3] Recently, some silica-based zeolites analogous materials,[4] fluorinated amporphous carbon,[5] benzoxazine-based polymers[6] have been used for low dielectric constant material as interlayer dielectrics.

Metal-organic-frameworks (MOFs) represent a subsystem of highly order nanoporous crystalline coordination polymer, and have widely studied for their applications in gas storage,[7] sensing,[8] catalysis[9] and drug delivery.[10] MOFs are the promising low dielectric constant material because they have well-defined monodisperse porosity.[11] However the dielectric properties of MOFs materials have been rarely investigated to date.[12,13] Theoretical calculation indicated that the static dielectric constant values of some MOFs materials is less than 2.[14] These calculations did not take into the molecule orientational and ionic contributions to the molecular polarizability, which mainly contributions to the dielectric constant. To the best of our knowledge, almost all of the MOFs materials with low dielectric constant is due to removal of guest molecules.[15] Usually, the guest molecules in MOFs materials are easily movable owing to their weak interaction with the framework, and the dipole motion of the polar guest molecules probably produce significant dielectric response and interesting dielectric properties.[16]

In this work, we report the first 3D hydrogen-bonding metal-organic frameworks with a formula $[Zn(CEIC)_2(H_2O)]\cdot$ 2DMF (compound **1**, where CEIC = 4-carboxy-2-ethyl-1H-imidazole-5-carboxylate) shows low dielectric constant value at high temperature. The novel dielectric relaxation of this compound was observed.

The reaction of 2-ethyl-4H-imidazole-4,5-dicarbonitrile (EIDN) and $Zn(NO_3)_2\cdot 6H_2O$ in 4:1 mol ratio in 20 ml DMF (N, N,-dimethylformamide), then 6 ml distilled water was added and sealed in Teflon-lined autoclave and heated to 80 ^{O}C for 48 h. The insoluble product was removed by filtration and the solution was slowly evaporated at room temperature. Colorless block-shape crystals were obtained after 7 days in solution. The phase purify of **1** was confirmed by PXRD and elemental analysis (Figure S1).

Crystal of **1** at room temperature belongs to monoclinic space group C2/c. The asymmetric unit of **1** is shown in Figure 1a, it can be seen that the Zn(II) ion is five-coordinated with two oxygen atoms(O1, O1A) and two nitrogen atoms (N1, N1A) from two CEIC ligands and one oxygen atom (O1W) from one water molecule to give the ZnO_3N_2 distorted trigonal-bipyramidal geometry. The zinc ions, N1 and N2 atoms are all situated on a center of inversion. The coordinated H_2O and free DMF molecules are order in this temperature. It should be noted that there are complicated H-bonding systems between CEIC ligand, H_2O and DMF molecules (Figure S2, Figure S3). Parallel to the (1, 0, 1) plane, the isolated $[Zn(CEIC)_2(H_2O)]$ unit are connected to each other via the multifurcated intermolecular O···O interactions forming one-dimension (1D) chain with shorter interatomic separations, 2.753 Å of O(2)···O(3), 2.980 Å of O(2)···O(3)^{i} (symmetric code: i =0.5- x, -10.5-y, -1-z, ref. Figure 1b). The H atoms of H_2O make a link with adjacent parallel chain via O-H···N H-bonding to form 2D layer. Furthermore, along the c-axis direction, each coordinated H_2O molecules can serve as a three-connected node to provide two H atoms to two N atoms of two $[Zn(CEIC)_2]$ units forming 3D supramolecular hydrogen-bonding framework with 1D lipophilic

[a] *School of Environmental Science, Nanjing Xiaozhuang University, Nanjing 211171, P.R.China*
E-mail: duanhaibao4660@163.com
†Electronic Supplementary Information (ESI) available:experimental details, additional figures, power XRD and TG curves.For ESI or other electronic format See DOI: 10.1039/x0xx00000x

square-shape channels (with H-bonding parameters: $d_{O(1w)\cdots N(2)ii}$ = 2.715 Å, $d_{H(1w)\cdots N(2)ii}$ = 2.124 Å, ∠O(1W)-H(1W)···N(2)^{ii} = 174.53. symmetric code ii = -0.5+x, 0.5+y, 1+z), where the guest DMF molecules are located in 1D channel (Figure 1c). The size of the channel considering the van der Walles radii is about 7.8×7.8 Å^2. TG results indicated the first step weight loss is ca. 25.2% between 100 and 170 ^{O}C, corresponding to losing two lattice DMF molecules (calc. 24.5%); the second gradually weight loss is ca. 27.2% between 170 and 210 ^{O}C, corresponding to losing one coordinated water molecules (calc. 27.5%) (Figure 1d). After complete removal of the coordinated water molecules from Zn ions, the framework is decomposed.

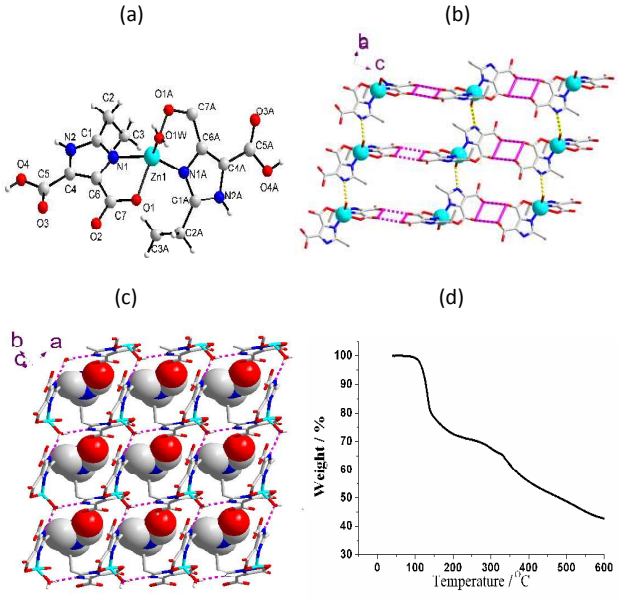

Figure 1 (a) Molecular structure in an asymmetric of **1** at 296 K (DMF molecule was omitted for clarity); (b) 1D chains in the structure of **1**, and their interconnected into 2D sheets though hydrogen bonding between chains; (c) 3D framework structure of **1**, showing the DMF molecules (space-filling models) occupying the cavity; (d) plot of TG cure of **1** over the temperature of 25-600^{O}C.

Frequency dependences of dielectric permittivity (*ε'*) and dielectric loss tan*(δ)* = *ε''* / *ε'* are shown in Figure 2 for **1** in the temperature range 30-165 ^{O}C and in the frequency range of 1-10^6 Hz. It is clear that dielectric permittivity of compound **1** is between 3.98 and 3.90 at the frequencies between 100 and 10^6 Hz at 30 ^{O}C, while the dielectric loss is 0.0039-0.0019 (Figure 2a and 2b), which indicated dynamic polar molecules motion in the **1** can not follow the applied electric field beyond which the dipole remain freeze with no effective contribution the dielectric permittivity at such temperature. It is very interesting as the temperature increase from 30 to 90 ^{O}C, dielectric permittivity increases slowly. Dielectric permittivity of **1** at 90 ^{O}C is between 4.20 and 3.98 at the frequency range of 100-10^6 Hz. Usually, the MOF materials with low dielectric permittivity value feature the reorientation motions of polar guest molecules being restricted at low temperature or frameworks solvent-free.[12,17] TG results indicated no obvious weight loss is observed before 90 ^{O}C in **1**, which indicated that the polar DMF and water molecules are still contributing to dielectric permittivity at such temperature. Though polar DMF and water molecules get enough excitation thermal energy at the high temperature, and the reorientation dynamics of them is activated. We think that the low dielectric permittivity of **1** in the high temperature is attributed to partially canceled polarization of DMF and water molecules by each other, which thus lead to small increase of dielectric permittivity. As indicated by the crystal structure, the orientation of the dipole moment of DMF and water molecules is very different. Up to date, the MOF materials with low dielectric constant have been reported,[17] and to the best of our knowledge, compound **1** with polar solvent molecules is a very rare example to show low dielectric constant at high temperature. As the temperature further increases, the DMF molecules are gradually removed, and the dielectric permittivity value rapidly increase, indicating that after removing the polar guest DMF molecules, the thermally assisted dynamical dipole motion due to water molecules in the **1** will be appeared. In *ε' versus* T and *ε'' versus* T plots of **1** at selected frequency, a typical dielectric relaxation was observed in the temperature range of 110-160 ^{O}C (Figure 2c and 2d). The dielectric constant remains stable below 100 ^{O}C and then it displays a pronounced change to high dielectric states with a step-like anomaly depending on the frequency. The different models of mechanisms lead to the resonance dielectric relaxation spectra in the case of electronic polarization or molecular vibrations which occur at frequencies beyond 10^{12} Hz. At below this frequency, the dielectric relaxation spectra prevail relating to the behavior of dipole motion or ionic polarization. Therefore, the relaxation that appears in 1-10^6 Hz of **1** could be attributed to dipole motion of coordinated water. In order to eliminate the problem of the electrode polarization and space charge injection phenomena. The dielectric relaxation spectra of **1**, transformed into electric modulus spectra in Figure 2e by using Eq.(1), the dielectric modulus representation minimizes the unwanted effects of the extrinsic relaxation .

$$M'(\omega) = \frac{\varepsilon'}{\varepsilon'^2 + \varepsilon''^2} \qquad M''(\omega) = \frac{\varepsilon''}{\varepsilon'^2 + \varepsilon''^2} \quad (1)$$

It is observed that the maximum in M'' peak shift to higher frequency with the temperature increases. This implies that the polarization can be re-developed at high temperature, and thus the relaxation occurs in high frequency. In order to get the deep insights into the dielectric relaxation process, the frequency-dependence of peak for the M'' at different temperature is plotted (Figure 2f) and the following relation is:

$$\tau = \tau_0 \exp(\frac{E_a}{k_B T}) \quad (2)$$

Where $\tau = 1/f_{max}$ and f_{max} is the frequency at maximum in the plot of M''-f under different temperature; τ_0 represents the characteristic macroscopic relation time, E_a is the activation energy or potential barrier required for the dielectric relaxation, k_B is Boltzmann's constant. The best fits giving the following results using Eq.(2): τ_0= 6.729 (7) X 10^{-13} s and E_a = 121.80 (2) KJ / mol.

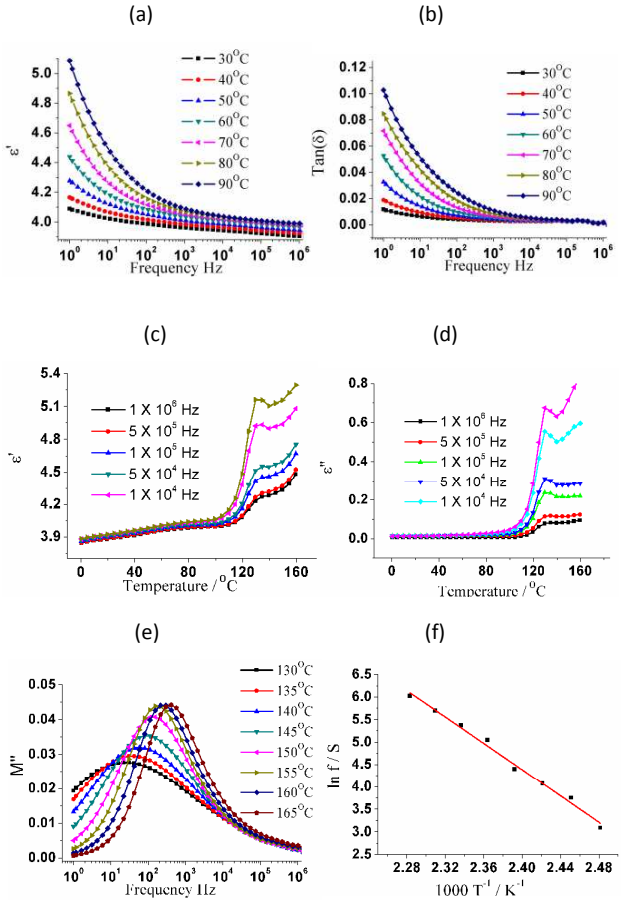

Figure 2 (a) and (b) Frequency dependencies of the ε' and ε'' of **1** in the 30-90 °C temperature range; (c) and (d) Temperature dependencies of ε' and *tan (δ)* of **1** in the 1-10^6 Hz frequency range; (e) Frequency dependencies of M'' in the 130-165°C temperature range; (f) Plots of ln *f versus* 1/T for the dielectric relaxation processes.

To further investigated the dielectric behavior of compound **1**, complex impedance (Z'-Z'') plot at different temperature was used. The impedance curves can be fitted by the equivalent circuit using the Zview fitting program where each impedance semicircle can be represent by a resistor, R, and capacitor, C, in parallel. The impedance curves in Figure 3a intercept zero at 30 °C and the order of magnitude of the capacitor is pF·cm^{-1}, which is due to the intrinsic behavior of the bulk materials.[18] The best fit gave σ_{dc} = 1.58 ×10^{-12} S•cm^{-1} at 30 °C. Such low σ_{dc} value indicated compound has insulating characteristics which are required for low-κ materials. It is clearly seen from the Figures S4 that the radius of semicircle decreases with increasing temperature, which indicates that the decrease of the bulk resistance with an increase of temperature. The temperature dependent conductivities σ_{dc} are plotted in the form of lnσ_{dc} versus 1000/T, as shown in Figure Figure 3b, the lnσ_{dc} as a function of 1000/T shows linear relationship in the temperature range of 135-160 °C, and the activation energy (E_{dc}) was estimated as 311.9 KJ / mol.

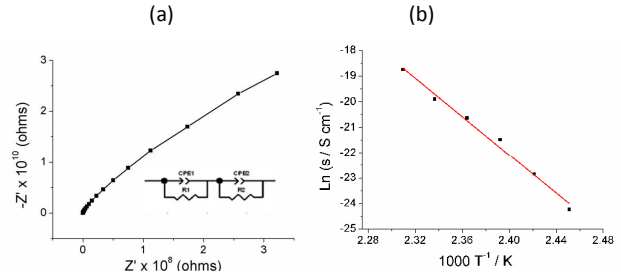

Figure 3 (a) Complex impedance of **1** at 30°C and (b) Arrhenius plots of **1** between 135 and 160 °C.

In summary, we have presented a 3D supramolecular hydrogen-bonding MOFs constructed by three-connected nodes coordinated H_2O molecules with 1D lipophilic channel, where the guest DMF molecules are located in channel. This compound shows dielectric constant value of less than 3.98 in the range of frequencies from 100 to 1 MHz and dielectric constant value of 4.20 at 90 °C, which is a very rare example to show low dielectric constant value at high temperature for the MOFs, and this is one of the few examples of the low dielectric constant MOF material with polar solvent molecule. Such low dielectric constant value is intrinsic behavior of the materials proved by complex impedance experiment. Our results suggested that the possibility of obtaining MOFs materials with low dielectric constant value at high temperature via the rationally designing channel and guest molecule.

The authors thanks Natural Science Foundation of High Learning Institutions of JiangSu Province and National Nature Science Foundation of China for their financial support (grant No: 13KJD150002, 21201103 and 21301093).

Notes and references

‡ Crystal data for compound **1**, $C_{20}H_{30}N_6O_{11}Zn$, M = 595.89, a = 11.5332(7)Å, b =10.5109(7)Å, c = 22.7132(15)Å, α = γ = 90.00°, β = 92.311(1)°, V = 2751.2(3)Å^3, Z = 4, D_c = 1.439 g·cm^{-3}. R_1= 0.0484, wR_2 = 0.1487. Single crystal diffraction data for **1** was collected on a Siemens SMART-CCD diffractometer with graphite monochromatic Mo Kα radiation (λ = 0.71073 Å). The structures were solved by direct method and refined on F2 using full matrix least-squares method with SHELXTL. Anisotropic thermal parameters were refined for the non-hydrogen atoms. The hydrogen atoms of the imidazole and alkyl chain were placed at calculated positions and those of the water molecule were located in difference Fourier maps.

[1] S. J. Martin, J. P. Godschalx, M. E. Mills, E. O. Schaffer and P. H. Townsend, Adv. Mater., 2000, **12,** 1769.
[2] W. C. Wang, R. H. Vora, E. Kang, K. G. Neoh, C. K. Ong and L. F. Chen, Adv. Mater., 2004, **16,** 54.
[3] W. Volksen, R. D. Miller and G. Dubois, Chem. Rev., 2010, **110,** 56.

[4] P. van der Voort, D. Esquivel, E. de Canck, F. Goethals, I. Van Driessche and F. J. Romero-Salguero, Chem. Soc. Rev., 2013, **42,** 3913; F. Goethals, I. Ciofi, O. Madia, K. Vanstreels, M. R. Baklanov, C. Detavernier, P. van der Voort and I. van Driessche, J. Mater. Chem., 2012, **22,** 8281.
[5] Y. Ma, H. Yang, J. Guo, C. Sathe, A. Agui and J. Nordgren, Appl. Phys. Lett., 1998, **72,** 3353.
[6] T. Fukumaru, T. Fujigaya, and N. Nakashima, Polym. Chem., 2012, **3,** 369.
[7] I. Hisaki, S. Nakagawa, N. Tohnai and M. Miyata, Angew. Chem. Int. Ed., 2015, **54,** 3008.; J. A. Mason, M. Veenstra and J. R. Long, Chem. Sci., 2014, **5,** 32; L. G. Li, S. F. Tang, C. Wang, X. X. Lv, M. Jiang, H. Z. Wu and X. B. Zhao, Chem. Commun., 2014, **50,** 2304; Z. J. Chen, K. Adil, L. J. Weseliński, Y. Belmabkhout and M. Eddaoudi, J. Mater. Chem. A, 2015, **3,** 6276; F. Gandara, H. Furukawa, S. Lee and O. M. Yaghi, J. Am. Chem. Soc., 2014, **136,** 5271.
[8] H. L. Jiang, Y. Tatsu, Z. H. Lu and Q. Xu, J. Am. Chem. Soc., 2010, **132,** 5586; W. L .Liu, L. H. Ye, X. F. Liu, L. M. Yuan, J. X. Jiang and C. G. Yan, CrystEngComm, 2008, **10,** 1395; X. Zhu, H. Y. Zheng, X. F. Wei, Z. Y. Lin, L . H. Guo, B. Qiu and G. N. Chen, Chem. Commun., 2013, **49,** 1276.
[9] D. B. Dang, P. Y. Wu, C. He, Z. Xie and C. Y. Duan, J. Am. Chem. Soc., 2010, **132,** 14321; J. Can ivet, S. Aguado, Y. Schuurman and D. Farrusseng, J. Am. Chem. Soc., 2013, **135,** 4195; P. Valvekens, E. D. Bloch, J. R. Long, R. Ameloot and D. E. D. Vos, Catalysis Today, 2014, **246,** 55; M. Yoon, R. Sriambalaji, K. Kim, Chem. Rev., 2012, **112,** 1196; P. García-garcía, M. Müller and A. Corma, Chem. Sci., 2014, **5,** 2979.
[10] P. Horcajada, R. Gref, T. Baati, P. K. Allan, G. Maurin, P. Couvreur, G. Fe´rey, R. E. Morris and C. Serre, Chem. Rev., 2012, **112,** 1232; J. Zhuang, C. H. Kuo, L. Y. Chou, D. Y. Liu, E. Weerapana and C. K. Tsung, ACS Nano, 2014, **8,** 2812.
[11] S. Eslava, L. P. Zhang, S. Esconjauregui, J. W. Yang, K. Vanstreels, M. R. Baklanov and E. Saiz, Chem. Mater., 2013, **25.** 27; M. Usman, S. Mendiratta and K. L. Lu, ChemElectroChem., 2015, DOI: 10.1002/celc.201402456
[12] P. C. Guo, Z.Y. Chu, X. M. Ren, W. H Ning and W. Q. Jin, Dalton Trans., 2013, **42,** 6603.
[13] Z. H. Sun, J. H. Luo, T. L. Chen, L. N. Li, R. G. Xiong, M. L. Tong and M. C. Hong, Adv. Funct. Mater. 2012, **22,** 4855; X. Q. Liang, F. Zhang, H. X. Zhao, W. Ye, L.S. Long and G. S. Zhu, Chem. Commun., 2014, **50,** 6513.
[14] K. Zagorodniy, G. Seifert and H. Hermann, Appl. Phys. Lett., 2010, **97,** 251905.
[15] P. C. Guo, T. Y. Chen, X. M. Ren, W. H. Ning and W. Q. Jin, New J. Chem., 2014, **38,** 2254; M.Usman, C. H. Lee, D. S. Hung, S. F. Lee, C. C. Wang, T. T. Luo, L. Zhao, M. K. Wu and K. L. Lu, J. Mater. Chem. C, 2014, **2,** 3762.
[16] X. Y. Dong, B. Li, B. B. Ma, S. J. Li, M. M. Dong, Y. Y. Zhu, S. Q. Zang, Y. Song, H. W. Hou and T. C. W. Mak, J. Am. Chem. Soc., 2013, **135,** 10214; W. Zhang, H. Y. Ye, R. Graf, H. W. Spiess, Y. F. Yao, R. Q. Zhu and R. G. Xiong, J. Am. Chem. Soc., 2013, **135,** 5230; M. Sánchez-Andújar, S. Yáñez-Vilar, B. Pato-Doldán, C. Gómez-Aguirre, S. Castro-García, and M.A. Señarís-Rodríguez, J. Phys. Chem. C, 2012, **116,** 13026.
[17] M. Usman, S. Mendiratta and K. L .Lu, ChemElectroChem, 2015, DOI: 10.1002/celc.201402456; S. Mendiratta, M. Usman, T. Tseng, T. T. Luo, S. F. Lee, S. S. Sun, Y. C. Lin and K. L. Lu, Eur. J. Inorg. Chem., 2015, DOI: 10.1002/ejic.201403243.
[18] D. C. Sinclair, T. B. Adams, F. D. Morrison and A. R. West, Appl. Phs. Lett., 2002, **80,** 2153.